MDPI

Article

A Numerical Study on Chloride Diffusion in Cracked Concrete

Qiannan Wang [1], Guoshuai Zhang [1], Yunyun Tong [1,*] and Chunping Gu [2,3]

1   School of Civil Engineering and Architecture, Zhejiang University of Science and Technology, Hangzhou 310023, China; wangqiannan@zust.edu.cn (Q.W.); 212002814023@zust.edu.cn (G.Z.)
2   College of Civil Engineering, Zhejiang University of Technology, Hangzhou 310023, China; guchunping@zjut.edu.cn
3   Zhejiang Construction Investment Group, Hangzhou 310013, China
*   Correspondence: 112013@zust.edu.cn

Abstract: The cracks in concrete are a fast transport path for chlorides and influence the service life of concrete structures in chloride environments. This study aimed to reveal the effect of crack geometry on chloride diffusion in cracked concrete. The chloride diffusion process in cracked concrete was simulated with the finite difference method by solving Fick's law. The results showed that the apparent chloride diffusivity was lower in more tortuous cracks, and the cracks with more narrow points also showed lower apparent chloride diffusivity. For tortuous cracks, a higher crack width meant relatively more straight cracks, and consequently, higher apparent chloride diffusivity, while a lower crack width resulted in more tortuous cracks and lower apparent chloride diffusivity. The crack depth showed a more significant influence on the chloride penetration depth in cracked concrete than crack geometry did. Compared with rectangular and V-shaped cracks, the chloride diffusion process in cracked concrete with a tortuous crack was slower at the early immersion age. At the same crack depth, the crack geometry showed a marginal influence on the chloride penetration depth in cracked concrete during long-term immersion.

Keywords: cracked concrete; crack width; crack depth; tortuosity; numerical simulation

1. Introduction

In chloride environments such as marine areas, the chloride diffusivity of concrete is considered to be the key point that determines the service life of reinforced concrete structures [1–3]. The chloride concentration threshold value that initiates the corrosion process is designated as the critical chloride concentration with respect to the binder content [4]. This value is usually taken in the range of 0.5–0.9% for tidal and splash zones, and 1.6–2.3% for submerged structures [5]. Normally, cracks always exist in concrete due to shrinkage, external load or other reasons [6,7]. The crack in concrete could act as a path for the fast transport of chlorides, thus accelerating the chloride transport in concrete [8].

Numerous experimental studies have shown that the chloride diffusivity in cracked concrete is significantly influenced by the crack geometry [9,10]. Crack width is regarded as the most important factor that influences the chloride diffusivity in cracked concrete [8]. General findings on this topic have been obtained [11–13]. The chloride diffusivity in a concrete crack is not influenced by the crack width when the crack width is very small (smaller than a low threshold). Under this circumstance, the cracks do not act as a fast transport path for chlorides, and the chloride diffusivity in concrete cracks is close to that in sound concrete. When the crack width is very large (bigger than a high threshold), the chloride diffusivity in a concrete crack is also independent of the crack width. The chlorides could be transported very quickly in the cracks, and the chloride diffusivity in concrete cracks is considered to be equal to the chloride diffusivity in bulk crack solution. When the crack width is between the low and high thresholds, the chloride diffusivity is obviously influenced by the crack width. However, the values for the low and high

thresholds, and the relationships between the chloride diffusivity in a concrete crack and crack width, varied in previous studies [8].

Djerbi et al. [14] adopted a steady-state migration test to study the influence of crack width on chloride diffusivity in cracked concrete. The chloride diffusivity in concrete cracks was also calculated in their study, and the relationship between the chloride diffusivity in concrete cracks and crack width was established. The low and high thresholds in their study were 30 μm and 80 μm, respectively, and the calculated chloride diffusivity in concrete cracks increased linearly with the crack width when the crack width was between 30 μm and 80 μm. Non-steady-state migration and diffusion methods were adopted by several researchers to study the effect of crack width on the chloride diffusivity in concrete crack [15,16]. The low threshold ranged from 30 μm to 120 μm, and the high threshold was between 80 μm and 680 μm. There is still no consensus on the exact values of the low and high thresholds. The different concrete compositions, crack generation methods and chloride diffusion test methods may be the reasons for the different results.

In addition to the crack width, the crack depth, tortuosity, connectivity and surface roughness could also influence the chloride transport process [17–21]. Marsavina et al. [22] found that the chloride penetration depth increased with an increasing (artificial) crack depth. This effect was more pronounced for longer test durations. Similar results were also found by Audenaert [13]. The chloride diffusivity in real concrete cracks was lower than that in artificial rectangular cracks and V-shaped cracks, and the chloride diffusivity in C30 cracks was higher than that in C80 cracks [11]. This was mainly because the cracks in concrete with a low water-to-binder ratio may be blocked due to the self-healing phenomenon, thus hampering the chloride transport process [23].

Due to the uncertainties during experimental studies, especially the geometry of the induced cracks in concrete, the influence of crack geometry on chloride diffusivity in concrete cracks has not been clearly revealed yet. In experimental studies, the crack geometry cannot be controlled when introducing real cracks in concrete, and human influences always exist when experiments are performed. For example, when studying the effect of crack width, cracks with the same width at the concrete surface could be created, but the crack geometry will vary in different concrete specimens. Hence, it is difficult to systemically study the effect of geometry on chloride diffusion in cracked concrete with experiments. Under this circumstance, numerical methods could provide a more promising solution to this question [8]. With simulation studies, experimental errors can be eliminated, and cracks with desired geometries can be implemented in the simulations. In this study, the chloride diffusion process in cracked concrete was simulated. The apparent chloride diffusivity in concrete cracks with different geometries was calculated, and the effect of crack geometry on the chloride diffusion in cracked concrete was discussed.

2. Simulation Methods

2.1. Numerical Method

The chloride diffusion process in cracked concrete follows the mass conservation equation and Fick's diffusion law [1]. In general, the chloride diffusion process in cracked concrete can be described as follows:

$$\frac{\partial C}{\partial t} = div(D \cdot gradC) \tag{1}$$

where C is the chloride concentration, t is time and D is the chloride diffusivity in sound concrete or crack solution.

To overcome the computational limitations, the chloride transport process in concrete can be simulated with simplified 2D elements [24]. For the case of 2D, Equation (1) becomes:

$$\frac{\partial C}{\partial t} = \frac{\partial C}{\partial x}(D\frac{\partial C}{\partial x}) + \frac{\partial C}{\partial y}(D\frac{\partial C}{\partial y}) \tag{2}$$

The Crank–Nicholson finite difference method was used to solve Equation (2). The finite difference approximation of Equation (2) can be written as follows:

$$
\begin{aligned}
\frac{C_{i,j}^{n+1} - C_{i,j}^n}{\Delta t} =& \frac{D_{(i+1)/2,j}C_{i+1,j}^n - \left(D_{(i+1)/2,j} + D_{(i-1)/2,j}\right)C_{i,j}^n - D_{(i-1)/2,j}C_{i-1,j}^n}{2 \times (\Delta x)^2} \\
&+ \frac{D_{(i+1)/2,j}C_{i+1,j}^{n+1} - \left(D_{(i+1)/2,j} + D_{(i-1)/2,j}\right)C_{i,j}^{n+1} - D_{(i-1)/2,j}C_{i-1,j}^{n+1}}{2 \times (\Delta x)^2} \\
&+ \frac{D_{i,(j+1)/2}C_{i,j+1}^n - \left(D_{i,(j+1)/2} + D_{i,(j-1)/2}\right)C_{i,j}^n - D_{i,(j-1)/2}C_{i,j-1}^n}{2 \times (\Delta y)^2} \\
&+ \frac{D_{i,(j+1)/2}C_{i,j+1}^{n+1} - \left(D_{i,(j+1)/2} + D_{i,(j-1)/2}\right)C_{i,j}^{n+1} - D_{i,(j-1)/2}C_{i,j-1}^{n+1}}{2 \times (\Delta y)^2}
\end{aligned}
\tag{3}
$$

where $C_{i,j}^n$ is the chloride concentration at nod (i,j) at time step n; $D_{i,j}$ is the chloride diffusivity at nod (i, j); $D_{(i+1)/2,j}$, $D_{(i-1)/2,j}$, $D_{i,(j+1)/2}$ and $D_{i,(j-1)/2}$ are the harmonic means of $D_{i+1,j}$ and $D_{i,j}$, $D_{i-1,j}$ and $D_{i,j}$, $D_{i,j+1}$ and $D_{i,j}$, $D_{i,j-1}$ and $D_{i,j}$, respectively [25]. By solving the implicit difference equations, the chloride concentration distribution in cracked concrete at different times, i.e., the chloride diffusion process, can be obtained. A self-written MATLAB (MathWorks, Natick, MA, United States) program was used to solve the diffusion equation. The Crank-Nicholson difference scheme is stable unconditionally, therefore, the numerical solutions are always convergent [26].

2.2. Simulation of the Steady-State Chloride Diffusion Process

In order to reveal the influence of crack geometry on the chloride transport in cracked concrete, steady-state diffusion in cracked concrete with different crack geometries was simulated. The flux through the outlet surface at a steady state can be determined and can then be used to calculate the chloride diffusivity in the specimen.

For a cracked concrete specimen, this method can be used to determine the chloride diffusivity in the cracks. This calculated chloride diffusivity is regarded as the apparent chloride diffusivity in crack D_{cr}', which is influenced by the crack geometry [11]. On the other hand, the chloride diffusivity in crack solution D_{cr} is independent of crack geometry but is determined, instead, by the characteristic of the crack solution [27].

Figure 1 shows a schematic illustration of the simulated steady-state diffusion in concrete with a crack in 2D. A 1 cm × 1 cm square is used to represent the cracked concrete specimen. The whole domain was digitized into a 1000 × 1000 mesh when performing the finite difference analysis. The initial chloride concentration at every nod was 0 mol/L. Dirichlet boundary conditions [25] were applied in the simulations. The chloride concentrations at the inlet surface ($x = 0$ mm) and outlet surface ($x = 10$ mm) were set to be 1 mol/L and 0 mol/L, respectively. The upper and lower surfaces were considered to be impermeable, which meant that chloride flux through these two surfaces was zero. A crack existed at the center of the specimen, and the chloride diffusivity in the crack solution D_{cr} was assumed to be 1.61×10^{-9} m^2/s, which is the chloride diffusivity in dilute NaCl solution at 25 °C [28]. In order to study the effect of crack geometry on the chloride diffusion in the crack, the chloride diffusivity in the sound concrete (D_0) was set to be zero for simplicity. The time-step was set to be 10^{-4} years.

The simulation in MATLAB program stopped when the chloride concentration in concrete stopped changing, which meant that steady-state diffusion had been achieved. Consequently, the chloride concentration distribution in this cracked concrete and the flux J through the outlet surface at a steady state could be determined through simulation.

The chloride diffusivity of the whole specimen D can be calculated according to Fick's law:

$$
D = \frac{J}{A}\frac{L}{\Delta C}
\tag{4}
$$

where A is the area of the outlet surface, L is the length of the specimen and ΔC is the chloride concentration difference between the inlet and outlet surfaces. Assuming that the sound concrete is impermeable, the chloride only diffuses through the crack. Therefore,

$$J_{cr} = J \tag{5}$$

where J_{cr} is the flux through the crack at a steady state and it can be calculated as follows:

$$J_{cr} = -D_{cr}\frac{\partial C_{cr}}{\partial x}\Big|_{x=outlet} A_{cr} \tag{6}$$

where A_{cr} is the area of the crack at the outlet surface. The flux J_{cr} and chloride concentration distribution can be obtained with the simulation. Based on Fick's law, the apparent chloride diffusivity in the crack D_{cr}' can be determined as follows:

$$D_{cr}' = \frac{J_{cr}}{A_{cr}}\frac{L}{\Delta C} \tag{7}$$

By substituting Equation (4) into Equation (5), the relationship between D_{cr}' and D_{cr} can be described as follows:

$$D_{cr}' = -D_{cr}\frac{\partial C_{cr}}{\partial x}\Big|_{x=outlet}\frac{L}{\Delta C} \tag{8}$$

It should be pointed out that, D_{cr}' may be equal to D_{cr} when the crack is a straight rectangle with parallel crack surfaces, which is almost impossible for cracks in real concrete structures. In other cases, D_{cr}' is lower than D_{cr}, and the difference between them is dependent on the crack geometry.
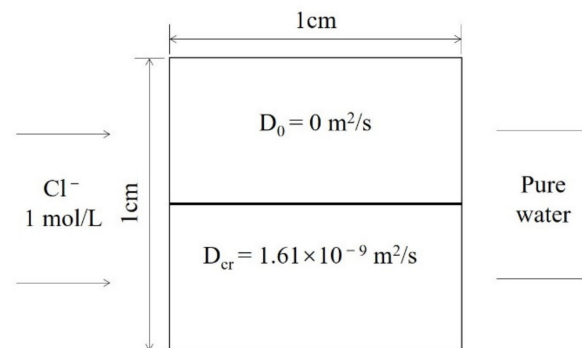

Figure 1. Illustration of the simulated steady-state diffusion in cracked concrete.

2.3. Simulation of Non-Steady-State Chloride Diffusion in Cracked Concrete

The chloride diffusion process in cracked concrete actually determines the service life of concrete structures in chloride environments. Assuming that a cracked concrete specimen is immersed in NaCl solution, an illustration of the simulation settings is shown in Figure 2. The whole domain was digitized into a 1000×500 mesh when performing the finite difference analysis. The initial and boundary conditions included the following: the chloride concentrations at the left surface and right surface were 0.555 mol/L and 0 mol/L, respectively, while other surfaces were sealed; the initial chloride concentration in the crack was considered to be 0.555 mol/L since the solution would enter into the crack due to capillary suction, and the initial chloride concentration in the concrete was set as 0 mol/L. The chloride diffusion process was also simulated by solving Equation (1) with the finite difference method. The chloride diffusivity in the sound concrete was set as 1.0×10^{-11} m^2/s, which is a typical value for widely used concrete with a water-to-binder ratio of over 0.45 [29]. The chloride diffusivity in crack solution D_{cr} was set to be 1.61×10^{-9} m^2/s [28]. The time-step was 10^{-4} years. The crack width at the

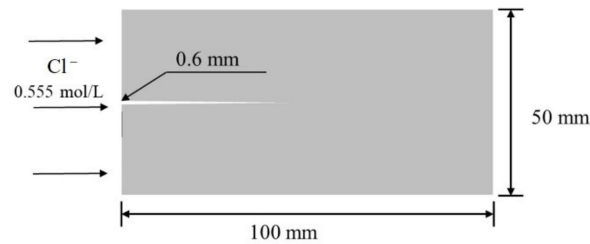concrete surface was 0.6 mm. Rectangular, V-shaped and real cracks were investigated in the simulation.

Figure 2. Illustration of the simulation settings for the non-steady-state chloride diffusion simulation in cracked concrete.

3. Results and Discussion

3.1. Effect of Crack Geometry on the Apparent Chloride Diffusivity in the Crack

In order to reveal the effect of crack geometry on the chloride diffusivity in concrete cracks, the chloride diffusion process in cracks with different widths and geometries was simulated. The input crack geometries are shown in Figure 3. Crack 1 was a straight crack with parallel crack surfaces. Crack 2 was a V-shaped crack with different widths at the chloride inlet and outlet surfaces. Cracks 3, 4 and 5 were tortuous cracks with folding lines as the crack surfaces. The tortuosity of these cracks followed the order of crack 5 > crack 4 > crack 3 > crack 1. Crack 6 was a real crack in C30 concrete from [30]. The crack width d ranged from 30 μm to 5 mm, and the width of crack 2 at the outlet end (d_1) was set to be 100 μm.
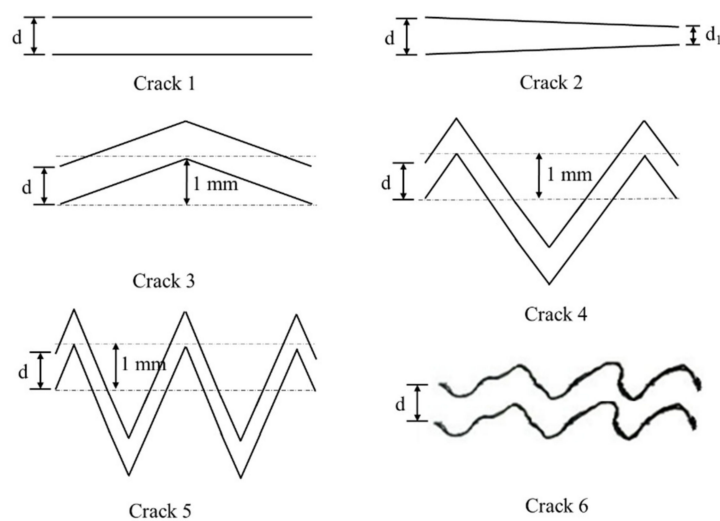

Figure 3. Crack geometries adopted in the simulation.

The apparent chloride diffusivity of the different cracks is shown in Figure 4. For the straight crack, the apparent chloride diffusivity in the crack was constant and equal to the chloride diffusivity in the crack solution. This means that the crack width did not influence the apparent chloride diffusivity in the straight crack. For the V-shaped crack, the apparent chloride diffusivity in the crack increased with the crack width at the inlet surface. It became a straight crack when the crack width at the inlet surface became 100 μm, which was equal to the width at the outlet surface. The apparent chloride diffusivity in the V-shaped crack kept increasing and exceeded the chloride diffusivity in crack solution when the crack width at the inlet surface was higher than 100 μm. This was because the higher crack width at the inlet surface led to higher chloride flux through the inlet and outlet surfaces, resulting in higher apparent chloride diffusivity in the crack.
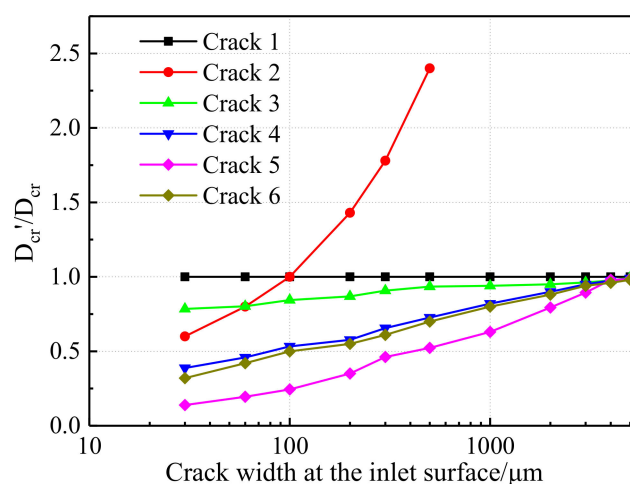
Figure 4. The effect of crack width on the apparent chloride diffusivity of concrete crack.

For tortuous cracks, the apparent chloride diffusivity in the cracks also increased with crack width, but it did not exceed the chloride diffusivity in crack solution. When the width of a tortuous crack was large enough (i.e., 5 mm), the apparent chloride diffusivity of the crack became close to the chloride diffusivity in crack solution. The large crack width made the tortuous crack similar to the straight crack with parallel crack surfaces. The apparent chloride diffusivity in the crack decreased with the increase in crack tortuosity. No matter how large the crack width was, the apparent chloride diffusivity in the cracks followed the order of crack 1 > crack 3 > crack 4 > crack 5. The results are in good agreement with findings obtained from experimental studies [11]. When the crack width was very small, the crack became more tortuous, and the apparent chloride diffusivity in the crack decreased. When the crack width was 30 μm, the apparent chloride diffusivities in cracks 3, 4 and 5 were 78%, 39% and 14% of the chloride diffusivity in crack solution, respectively. Hence, when the crack width is very small (e.g., <30 μm) and the crack geometry is complex, the chloride cannot diffuse quickly in the crack. The apparent chloride diffusivity in the crack would be close to that in sound concrete.

The real crack was also tortuous, and the apparent chloride diffusivity in the real crack was close to that of crack 4, which implies that real cracks could be simplified as fold-line cracks when simulating the chloride diffusion process. The detailed geometry of this fold-line necessitates further study to assure better agreement with reality. Moreover, the apparent chloride diffusivity in rectangular cracks was obviously higher than that in real cracks, especially when the crack width was under 1 mm. The apparent chloride diffusivity D_{cr}' in rectangular cracks is width-independent, while D_{cr}' in real cracks is governed by crack width.

When simulating the chloride diffusion process in cracked concrete, determination of the crack geometry and the chloride diffusivity in the crack is the most important aspect. Normally, in simulations, the crack geometry could be set as rectangular, V-shaped or real-shaped. If a real tortuous crack is simplified to be a rectangular crack, the chloride diffusivity in the crack should be width-dependent to reflect the effect of crack geometry on the chloride diffusivity [31].

In addition to the cracks shown in Figure 3, the chloride diffusion process in cracks with other geometries (as shown in Figure 5) was simulated. Cracks 7, 8 and 9 were tortuous cracks with narrow points. The width at the narrow points (d_2) was smaller than the crack width at the surface (d). In the simulation of chloride diffusion, d was set to be 100 μm, while the d_2 values were set as 20 μm, 40 μm, 60 μm and 80 μm, respectively, to investigate the effect of narrow points' width on the chloride diffusion in the cracks. The calculated apparent chloride diffusivities in the cracks with narrow points are shown in Figure 6.
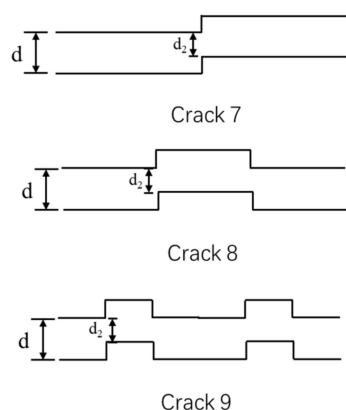
Figure 5. Geometries of tortuous cracks with narrow points adopted in the simulation.
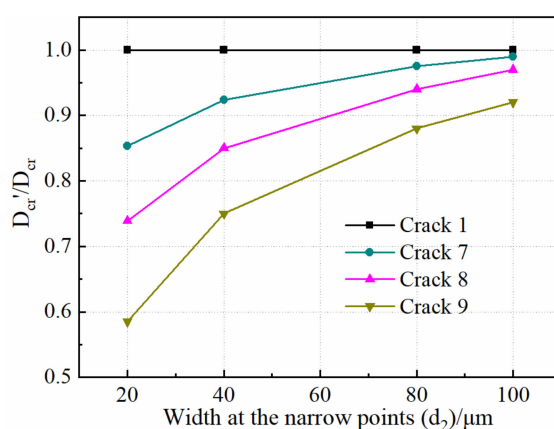

Figure 6. The apparent chloride diffusivity in cracks with narrow points.

For cracks with narrow points, the apparent chloride diffusivity decreased with the reduced width at the narrow points. For example, in crack 7, when the narrow point was 80 μm wide, the apparent chloride diffusivity in the crack was slightly lower than the chloride diffusivity in crack solution, whereas when the width of the narrow point was 20 μm, the apparent chloride diffusivity in the crack reduced to about 85% of the chloride diffusivity in crack solution. In addition, with more narrow points existing in the crack, the reduction in apparent chloride diffusivity with the reduced width at the narrow points was more significant. As for crack 8, the apparent chloride diffusivity in the crack was lower than that in crack 7; it decreased to 74% of chloride diffusivity in crack solution when the narrow points were 20 μm wide. The apparent chloride diffusivity in crack 9 was 59% of chloride diffusivity in crack solution when the width of the narrow points was 20 μm. It was, therefore, obvious that the narrow points in the cracks also showed a significant influence on the apparent chloride diffusivity in cracks.

Based on the simulations of the steady-state diffusion process, it can be concluded that the crack geometry, including the crack width, tortuosity and narrow points, showed a great impact on the apparent chloride diffusivity in cracks. When the chlorides enter the narrow points, the interaction between the crack surface and the chloride will be more pronounced and will hinder the fast diffusion of chlorides [32].

When the width of a real crack is small, the crack is generally more tortuous and has more narrow points. Therefore, the apparent chloride diffusivity in the crack will be very small, and may be close to the chloride diffusivity in sound concrete. When the crack width is large enough, the crack is more like a straight crack, whose apparent chloride diffusivity is close to the chloride diffusivity in crack solution.

3.2. Effect of Crack Geometry on the Chloride Diffusion Process in Cracked Concrete

The non-steady-state chloride diffusion process in cracked concrete was simulated using the finite difference method. Rectangular, V-shaped and real cracks were adopted in the simulations. The detailed geometries of these cracks are shown in Figure 7. The rectangular cracks had different crack depths (i.e., 25 mm, 35 mm and 45 mm). The depth of the V-shaped and real cracks was set to be 45 mm. The geometry of real crack was adopted from [33]. All of the cracks had a crack width of 0.6 mm at the left surface of the specimen.
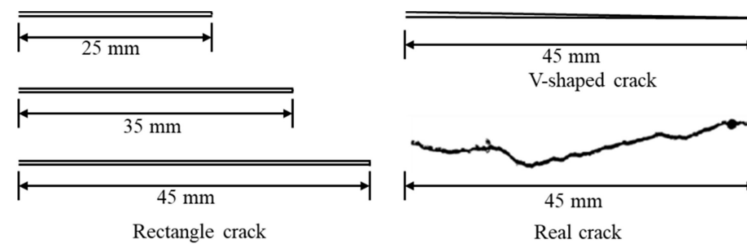

Figure 7. The crack geometries used in non-steady-state diffusion simulation (crack width at the left surface: 0.6 mm).

The simulated chloride concentration distributions in concrete with rectangular cracks after one year of immersion in NaCl solution are shown in Figure 8. The chloride penetrated the concrete specimen quickly through the crack, and the chloride penetration depth was largely dependent on the crack depth. A higher crack depth led to a deeper chloride penetration depth. Hence, the crack depth is the key factor that influences the service life of concrete structures in chloride environments. The chlorides also penetrated concrete through the crack surfaces; hence, the chloride concentration in concrete near the crack surfaces was also increased due to the presence of cracks.
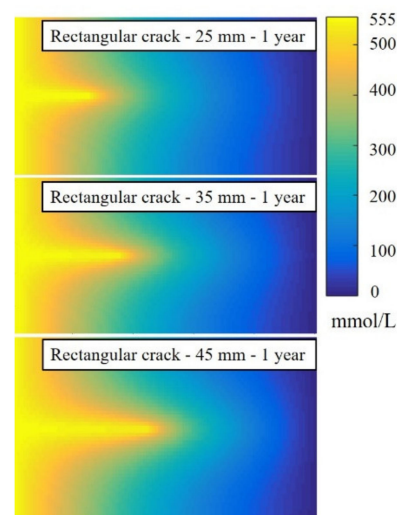

Figure 8. The simulated chloride concentration in cracked concrete with rectangular cracks after one year of immersion in NaCl solution.

The chloride concentration distributions in cracked concrete with different crack geometries are shown in Figure 9. At the immersion age of 0.01 years, it was quite obvious that the chloride concentration in the real tortuous crack was lower than that in the rectangular and V-shaped cracks. The tortuous crack inhibited the fast chlorides' diffusion in concrete cracks. When the immersion age increased, the chloride concentration distributions in different cracked concretes were close to each other. The chloride concentrations at the height of 25 mm in cracked concrete (i.e., at the center of the cracked concrete in the vertical direction) are shown in Figure 10. At the immersion age of 0.01 years, the

chloride concentration at the real crack tip was much lower than that in the rectangular and V-shaped cracks, and for the real crack, the chloride concentration beyond the crack tip was also lower than that in the other two. At the immersion age of one year, the chloride concentration distributions in cracked concrete with rectangular and V-shaped cracks were almost the same. The chloride concentration in the real crack was only slightly lower than that in the rectangular and V-shaped cracks. This suggested that the crack geometry influenced the chloride diffusion process in cracked concrete soon after the chloride penetrated the crack. However, for a long-term immersion with a given crack depth, the crack geometry did not show much influence on the chloride penetration depth in cracked concrete. In comparison, the influence of crack depth was more significant than that of crack geometry on the chloride penetration depth in cracked concrete in the long term.
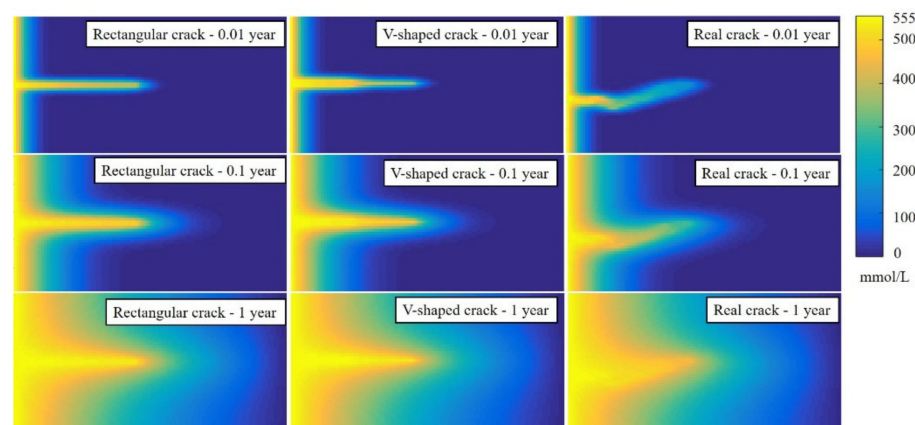

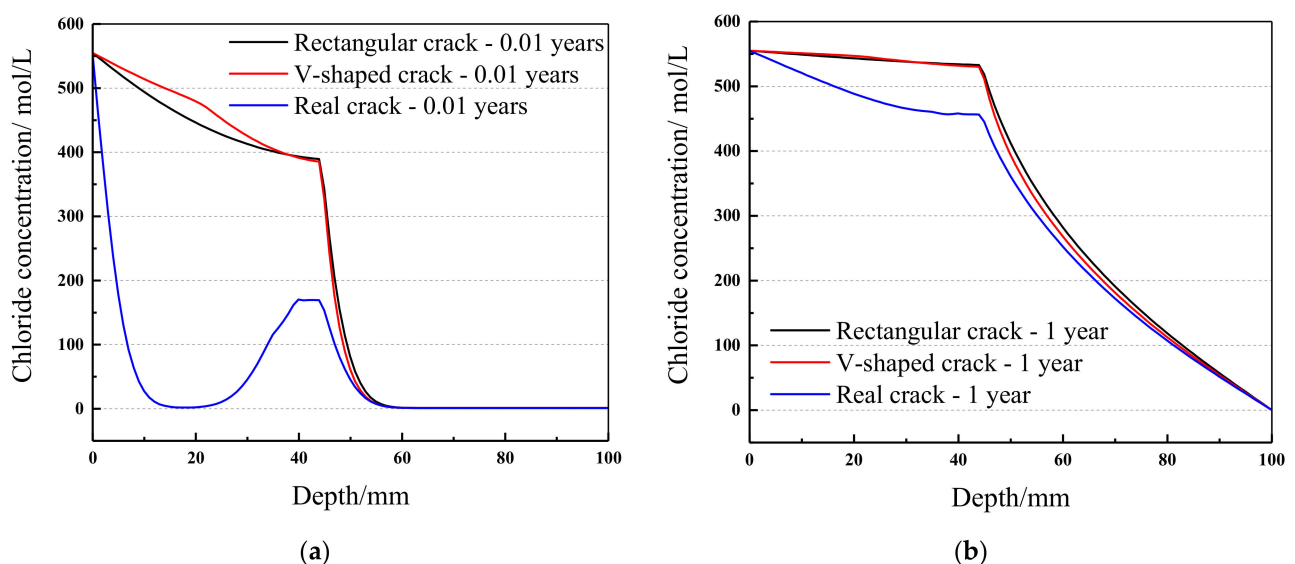**Figure 9.** The chloride concentration distribution in concrete with different crack geometries.

(**a**)

(**b**)

Figure 10. The chloride concentrations at the height of 25 mm in cracked concrete: (**a**) at the immersion age of 0.01 years; (**b**) at the immersion age of one year.

Generally, in cracked concrete, the crack width influences the short-term chloride diffusion process, but for long-term chloride diffusion, the influence of crack depth is more significant. That is, the crack depth is the main factor that influences the residual service life of a cracked concrete structure in chloride environments. Moreover, when predicting the residual service life of cracked concrete structures with numerical methods, the real crack could be simplified as rectangular (or other shaped) crack in the simulations.

4. Conclusions

Based on the simulations of steady and non-steady states of chloride diffusion in cracked concrete, the effects of crack geometry on the chloride diffusion behavior in cracked concrete were discussed. The following conclusions can be drawn.

(1) The apparent chloride diffusivity was lower in more tortuous concrete cracks. In addition, the narrow points in the cracks also showed a significant influence on the apparent chloride diffusivity in the cracks.

(2) When the crack width was very large, the apparent chloride diffusivity in tortuous cracks became almost equal to that in crack solution. When the crack width was small and the crack was more tortuous, the apparent chloride diffusivity in the crack reduced remarkably.

(3) The crack depth showed a more significant influence on the chloride penetration depth in cracked concrete than crack geometry did.

(4) Compared with rectangular and V-shaped cracks, the chloride diffusion process in cracked concrete with a tortuous crack was slower at the early immersion age, whereas with the same crack depth for a long term, the crack geometry showed a marginal influence on the chloride penetration depth in cracked concrete.

Author Contributions: Conceptualization, Q.W. and C.G.; methodology, Q.W. and C.G.; software, C.G.; validation, G.Z. and Y.T.; writing—original draft, Q.W. and C.G.; writing—review and editing, G.Z. and Y.T. All authors have read and agreed to the published version of the manuscript.

Data Availability Statement: Data are contained within the article.

References

1. Yang, C.Y.; Li, L.; Li, J.P. Service life of reinforced concrete seawalls suffering from chloride attack: Theoretical modelling and analysis. *Constr. Build. Mater.* **2020**, *263*, 120172. [CrossRef]
2. Yang, D.H.; Li, G.P.; Yi, T.H.; Li, H.N. A performance-based service life design method for reinforced concrete structures under chloride environment. *Constr. Build. Mater.* **2016**, *124*, 453–461. [CrossRef]
3. Zhang, J.Z.; Huang, J.; Fu, C.Q.; Huang, L.; Ye, H.L. Characterization of steel reinforcement corrosion in concrete using 3D laser scanning techniques. *Constr. Build. Mater.* **2020**, *270*, 121402. [CrossRef]
4. Reiterman, P.; Keppert, M. Effect of various de-icers containing chloride ions on scaling resistance and chloride penetration depth of highway concrete. *Roads Bridges-Drogi i Mosty* **2020**, *19*, 51–64. [CrossRef]
5. Hájková, K.; Šmilauer, V.; Jendele, L.; Cervenka, J. Prediction of reinforcement corrosion due to chloride ingress and its effects on serviceability. *Eng. Struct.* **2018**, *174*, 768–777. [CrossRef]
6. Yu, H.F.; Lu, J.L.; Qiao, P.Z. Localization and size quantification of surface crack of concrete based on Rayleigh wave attenuation model. *Constr. Build. Mater.* **2021**, *280*, 120172. [CrossRef]
7. Fu, C.Q.; Fang, D.M.; Ye, H.L.; Huang, L.; Wang, J.D. Bond degradation of non-uniformly corroded steel rebars in concrete. *Eng. Struct.* **2021**, *226*, 111392. [CrossRef]
8. Gu, C.P.; Ye, G.; Sun, W. A review of the chloride transport properties of cracked concrete: Experiments and simulations. *J. Zhejiang Univ-Sci. A* **2015**, *16*, 81–92. [CrossRef]
9. Li, K.F.; Li, L. Crack-altered durability properties and performance of structural concretes. *Cement Concrete Res.* **2019**, *124*, 105811. [CrossRef]
10. Zhu, H.G.; Fan, J.C.; Pang, S.; Chen, H.Y.; Yi, C. The Depth-Width Correlation for Shrinkage-Induced Cracks and Its Influence on Chloride Diffusion into Concrete. *Materials* **2020**, *13*, 2751. [CrossRef]
11. Ismail, M.; Toumi, A.; François, R. Effect of crack opening on the local diffusion of chloride in cracked mortar samples. *Cement Concrete Res.* **2008**, *38*, 1106–1111. [CrossRef]
12. Yoon, I.S.; Schlangen, E. Experimental examination on chloride penetration through micro-crack in concrete. *KSCE J. Civ. Eng.* **2014**, *18*, 188–198. [CrossRef]
13. Audenaert, K.; Schutter, G.D.; Marsavina, L. Influence of cracks and crack width on penetration depth of chlorides in concrete. *Eur. J. Environ. Civ. Eng.* **2009**, *13*, 561–572. [CrossRef]
14. Djerbi, A.; Bonnet, S.; Khelidj, A.; Baroghel-bouny, V. Influence of traversing crack on chloride diffusion into concrete. *Cement Concrete Res.* **2008**, *38*, 877–883. [CrossRef]

15.   Rodriguez, O.G.; Hooton, R.D. Influence of cracks on chloride ingress into concrete. *ACI Mater. J.* **2003**, *100*, 120–126.
16.   Weiss, J.; Couch, J.; Pease, B.; Laugesen, P. Influence of Mechanically Induced Cracking on Chloride Ingress in Concrete. *J. Mater. Civ. Eng.* **2017**, *29*, 04017128. [CrossRef]
17.   Benkemoun, N.; Hammood, M.N.; Amiri, O. A meso-macro numerical approach for crack-induced diffusivity evolution in concrete. *Constr. Build. Mater.* **2017**, *14*, 72–85. [CrossRef]
18.   Akhavan, A.; Rajabipour, F. Quantifying Permeability, Electrical Conductivity, and Diffusion Coefficient of Rough Parallel Plates Simulating Cracks in Concrete. *J. Mater. Civ. Eng.* **2017**, *29*, 04017119. [CrossRef]
19.   Yang, K.H.; Singh, J.K.; Lee, B.Y.; Kwon, S.J. Simple Technique for Tracking Chloride Penetration in Concrete Based on the Crack Shape and Width under Steady-State Conditions. *Sustainability* **2017**, *9*, 282. [CrossRef]
20.   Yang, K.H.; Cheon, J.H.; Kwon, S.J. Modeling of chloride diffusion in concrete considering wedge-shaped single crack and steady-state condition. *Comput. Concrete* **2017**, *19*, 211–216. [CrossRef]
21.   Ye, H.L.; Jin, N.G.; Jin, X.Y.; Fu, C.Q. Model of chloride penetration into cracked concrete subject to drying-wetting cycles. *Constr. Build. Mater.* **2012**, *36*, 259–269. [CrossRef]
22.   Marsavinaa, L.; Audenaertb, K.; Schutterb, G.D.; Faura, N.; Marsavinac, D. Experimental and numerical determination of the chloride penetration in cracked concrete. *Constr. Build. Mater.* **2009**, *23*, 264–274. [CrossRef]
23.   Xu, J.; Peng, C.; Wan, L.J.; Wu, Q. Effect of Crack Self-Healing on Concrete Diffusivity: Mesoscale Dynamics Simulation Study. *J. Mater. Civil. Eng.* **2020**, *32*, 04020149. [CrossRef]
24.   Šavija, B.; Luković, M.; Schlangen, M. Lattice modeling of rapid chloride migration in concrete. *Cem. Concr. Res.* **2014**, *61–62*, 49–63. [CrossRef]
25.   Ukrainczyk, N.; Koenders, E.A.B.; Vanbreugel, K. Morphological nature of diffusion in cement paste. In *Concrete Repair, Rehabilitation and Retrofitting*; Alexander, M.G., Beushausen, H.D., Dehn, F., Eds.; Taylor & Francis Group: London, UK, 2012; pp. 321–327.
26.   Song, H.W.; Shim, H.B.; Petcherdchoo, A.; Park, S.K. Service life prediction of repaired concrete structures under chloride environment using finite difference method. *Cem. Concr. Comp.* **2009**, *31*, 120–127. [CrossRef]
27.   Singh, M.B.; Dalvi, V.H.; Gaikar, V.G. Investigations of clustering of ions and diffusivity in concentrated aqueous solutions of lithium chloride by molecular dynamic simulations. *RSC Adv.* **2015**, *5*, 15328–15337. [CrossRef]
28.   Gu, C. Chloride Transport Property and Service Life Prediction of UHPFRCC under Flexural Load. Ph.D. Thesis, Southeast University, Nanjing, China, 2016. (In Chinese).
29.   Shafikhani, M.; Chidiac, S.E. Quantification of concrete chloride diffusion coefficient—A critical review. *Cem. Concr. Comp.* **2019**, *99*, 225–250. [CrossRef]
30.   Chen, S. Study on Transport Behavior of Chlorides in Concrete Cracks. Master's Thesis, Zhejiang University of Technology, Hangzhou, China, 2020. (In Chinese).
31.   Jin, W.L.; Yan, Y.D.; Wang, H.L. Chloride diffusion in the cracked concrete. In *Fracture Mechanics of Concrete and Concrete Structures—Assessment, Durability, Monitoring and Retrofitting of Concrete Structures*; Oh, B.H., Choi, O.C., Chung, L., Eds.; Korea Concrete Institute: Seoul, Korea, 2010; pp. 880–886.
32.   Maekawa, K.; Ishida, T.; Kishi, T. *Multi-Scale Modeling of Structural Concrete*; Taylor & Francis: Oxon, UK, 2009; pp. 291–352. [CrossRef]
33.   Ni, T.; Zhou, R.; Gu, C.; Yang, Y. Measurement of concrete crack feature with android smartphone APP based on digital image processing techniques. *Measurement* **2020**, *150*, 107093. [CrossRef]